$^{13}$C NMR data (CD$_2$Cl$_2$, 21 °C, $\delta$ relative to Me$_4$Si): 213.5 ($\mu$-C$_2$Me$_2$), 154.9, 140.2, 124.7 (NC$_5$H$_5$), 64.1, 57.0 ($\mu$-NMe$_2$), 22.2 ($\mu$-C$_2$*Me*$_2$).

**Crystallographic Studies.** General operating facilities and listings of programs have been given previously.[22] Crystal data for the three compounds studied in this work are summarized in Table X.

**W$_2$Cl$_2$(NMe$_2$)$_4$($\mu$-C$_2$H$_2$)(py)$_2$·CH$_2$Cl$_2$.** The sample used in the study was cleaved from a larger crystal and transferred to the goniostat by using standard inert-atmosphere handling techniques. A systematic search of a limited hemisphere of reciprocal space revealed a set of no systematic absences or symmetry, indicating a probable space group of P1̄. The structure was solved by a combination of direct methods (MULTAN 78) and Fourier techniques and refined by full-matrix least squares. All hydrogen atoms were located and refined.

A final Fourier was featureless, the largest peaks being 0.65 and 0.59 e/Å$^3$, located adjacent to the two metal positions.

**W$_2$Cl$_3$(NMe$_2$)$_3$($\mu$-PhC$_2$H)(py)$_2$·$^1$/$_2$C$_7$H$_8$.** The crystal used in the study was cleaved from a conglomerate and transferred to the goniostat by using standard inert-atmosphere techniques. A systematic search of a limited hemisphere of reciprocal space yielded a set of reflections which exhibited monoclinic symmetry and systematic extinctions corresponding to the space group P2$_1$/n.

The structure was solved by using a combination of direct methods and standard heavy-atom Fourier techniques. The W atoms were located by using MULTAN, and the remaining atoms were located in a difference Fourier phased with the W atoms. A subsequent difference Fourier indicated the presence of a solvent molecule situated at a center of symmetry. The asymmetric unit contains one molecule of W$_2$Cl$_3$(NMe$_2$)$_3$($\mu$-PhCCH)(py)$_2$ and one-half molecule of toluene. The crystal shape was quite irregular, and attempts at an absorption correction failed to improve the data. The hydrogen atoms were not located but were inserted in calculated positions and remained fixed during the least-squares refinements, where all other atoms were refined by using anisotropic thermal parameters. Attempts at locating the H atom on the acetylenic carbon atom failed (this H atom was omitted during refinements).

The final difference Fourier contained a few peaks of approximately 1.3 e/Å$^3$, they were located within 1.2 Å of the W atoms.

**W$_2$Cl$_4$(NMe$_2$)$_2$($\mu$-C$_2$Me$_2$)(py)$_2$.** A suitable crystal was cleaved from a larger mass and transferred to the goniostat by using standard inert-atmosphere handling techniques. It should be noted that there appeared to be two definite sizes of crystals present. The larger crystals (a fragment of which was used herein) were, in general, covered with a layer of much smaller diamond-shaped platelets. There was no evidence that the two forms were the same. The sample was cooled to −160 °C after transfer to the goniostat and characterized in the usual manner (space group P2$_1$/n, based on 24 close-in reflections).

The structure was solved by location of the tungsten atoms in a Patterson synthesis, followed by Fourier techniques. All atoms, including hydrogens, were located and refined (isotropic for H; anisotropic for W, N, and C). The hydrogen atoms, while qualitively correct, show a significant scatter from the idealized positions expected on the basis of normal sp$^3$ bonding. $\psi$ scans indicated absorption to be a problem, and the data were corrected accordingly. The residual dropped from $R(F)$ = 0.065 to 0.039 and $R_w(F)$ = 0.068 to 0.041 after the absorption correction was applied.

A final difference Fourier revealed four peaks of magnitude 0.9–1.5 e/Å$^3$ within 0.3 Å of the two tungsten atoms, and no other features were present. It should be noted that the thermal ellipsoids for C(7)–C(10) are somewhat "misshaped". A difference Fourier phased on all atoms, excluding C(7)–C(10), failed to indicate any disorder. We assume the large anisotropic shape is an artifact of the absorption correction as opposed to a thermal and/or disorder problem.

**Supplementary Material Available:** Tables of anisotropic thermal parameters and complete listings of bond distances and bond angles (5 pages); a listing of $F_o$ and $F_c$ (9 pages). Ordering information is given on any current masthead page. The complete structural reports are available in microfiche form only from the Indiana University Chemical Library at a cost of $2.50 per copy. Requires MSC Report No. 85005 for W$_2$Cl$_4$(py)$_2$(NMe$_2$)$_2$($\mu$-C$_2$Me$_2$), No. 84091 for W$_2$Cl$_3$(NMe$_2$)$_3$(py)$_2$($\mu$-PhC$_2$H)·$^1$/$_2$C$_7$H$_8$, and No. 85032 for W$_2$Cl$_2$(NMe$_2$)$_4$(py)$_2$($\mu$-C$_2$H$_2$)·CH$_2$Cl$_2$.

(22) Chisholm, M. H.; Folting, K.; Huffman, J. C.; Kirkpatrick, C. C. *Inorg. Chem.* **1984**, *23*, 1021.

# Stereoelectronic Causes of an Unusual Coordination Geometry of an Acetylene

Maria José Calhorda and Roald Hoffmann*

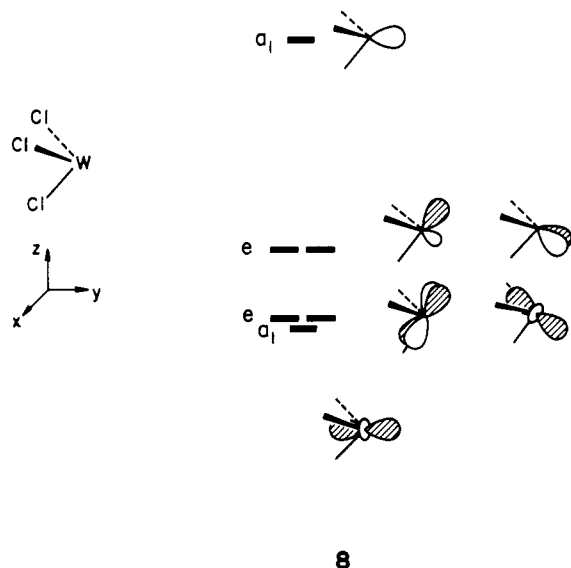*Department of Chemistry, Cornell University, Ithaca, New York 14853*

The recently synthesized W$_2$($\mu$-NMe$_2$)($\mu$-C$_2$Me$_2$)Cl$_4$(py)$_2$ complex is unique in featuring an acetylene twisted relative to the W–W axis to a geometry intermediate between parallel and perpendicular. Extended Hückel calculations provide an explanation for this deformation. In the perpendicular geometry one finds a small HOMO–LUMO gap, one which suggests, by a second-order Jahn–Teller argument, a twisting. This is true even in a hypothetical symmetrical environment, such as the hexachloride. But the potential energy minimum for one of the two twisted minima is much deepened by the asymmetric substitution. This effect can be traced to one metal–acetylene bonding orbital and is the result of a specific acetylene–carbon–chloride repulsive secondary interaction.
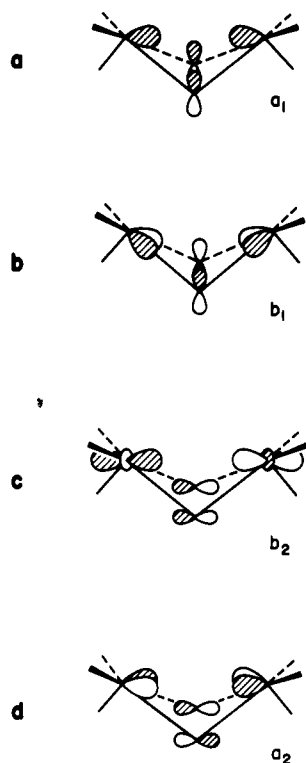
Until recently the myriad known dinuclear acetylene transition-metal complexes have fallen into two distinct

types: "perpendicular", 1, and "parallel", 2.[1] The distinction refers to the projected angle between the M–M

and C–C bonds, $\theta$ in **3**. Small deviations from the ex-



**1, perpendicular, $\theta \sim 90°$**    **2, parallel, $\theta \sim 0°$**



**3**

tremes of $\theta = 0$ or 90° are known, presumably due to crystal packing or unsymmetrical ligand environments. Larger deviations had been thought about[2] but had never been found, and the general body of experimental evidence argues for a large barrier to acetylene rotation.

The striking exception that has emerged in recent work by Ahmed, Chisholm, Folting, and Huffman is the ditungsten derivative $W_2(\mu\text{-NMe}_2)_2(\mu\text{-}C_2Me_2)Cl_4(py)_2$ (**4**). In



**4**

this $d^3$–$d^3$ complex the acetylene is most definitely twisted; $\theta = 55°$.[3] Furthermore there is an R–C–C–R torsion of 42°. **4** appears to be intermediate between **2** and **3** in several ways. We want to understand why such a distorted geometry for acetylene is favored in this particular tungsten environment. This study is based on extended Hückel calculations and symmetry arguments. Details about the calculations are to be found in the Appendix.

## Results and Discussion

The first step was to determine if the computational method we use mirrors the experimental result. We replaced the methyl groups on the acetylene, and those on the bridging amides by hydrogens, and simply rotated an acetylene (planar, HCC angle = 125°) relative to a frozen $W_2(NH_2)_2Cl_4py_2$ core. The resulting potential energy curve, one of several shown in Figure 1, clearly indicates a deep energy minimum near the observed structure. If in the unsymmetrical frame $\theta$ is defined as in **5**, so that



**5**

$\theta \simeq 125°$ corresponds to the observed structure, acetylene carbons point "toward" the pyridines. The position of the calculated minimum could be improved by allowing HCCH torsion.

(1) See references in: Hoffman, D. M.; Hoffmann, R; Fisel, C. R *J. Am. Chem. Soc.* **1982**, *104*, 3858.

(2) (a) Thorn, D. L.; Hoffmann, R. *Inorg. Chem.* **1978**, *17*, 126. (b) Hoffmann, D. M.; Hoffmann, R. *J. Chem. Soc. Dalton Trans.* **1982**, 1471.

(3) Ahmed, K. J.; Chisholm, M. H.; Huffman, J. D. *Organometallics* **1985**, *4*, 1312. Ahmed, K. J.; Chisholm, M. H.; Folting, K.; Huffman, J. C. *Organometallics*, preceding paper in this issue.

**Figure 1.** Change of total energy as the acetylene fragment is allowed to rotate around the $C_2$ symmetry axis in $W_2(NH_2)_2$-$(C_2H_2)Cl_6{}^{2-}$, $W_2(NH_2)_2(C_2H_2)Cl_4H_2{}^{2-}$, and $W_2(NH_2)_2(C_2H_2)Cl_4(py)_2$.

Given that the calculations yield the correct structural trend, we would like to understand why. To this end several other calculations were carried out, and these are the other curves in Figure 1. First we replaced a pyridine by a theoretician's dream, a hydride modeling the $\sigma$ donor and relatively neutral $\pi$ donor–aceptor capability of the pyridine ligand. This is **6**, $W_2(NH_2)_2(C_2H_2)Cl_4H_2{}^{2-}$. The



**6**                                        **7**

potential energy curve is similar to that for pyridine. Then we symmetrized the situation, by replacing the hydride or pyridine by chloride, **7**, $W_2(NH_2)_2(C_2H_2)Cl_6{}^{2-}$. Now the curve is symmetrical around 90°, as it must be, with two weak minima for twisted acetylenes. These are the trends we must understand.

### Bonding in Symmetrical $W_2(NH_2)_2(C_2H_2)Cl_6{}^{2-}$

We start from the orbitals of conical $ML_3$. They are derived from those of an octahedral $ML_6$ when three ligands (in a face) are removed, and have been described before.[4] They are shown in **8**. The higher energy $a_1$ orbital is essentially metal s and $y$. The next e set derives mainly from $xz$, $yz$ and $x,y$. These three orbitals are hybridized in such a way that they point to incoming ligands. The lower energy e and $a_1$ levels correspond to the $t_{2g}$ set of the parent octahedral molecule.

The next step is to interact two of these $WCl_3$ fragments.[2] While the process is similar to that described in ref 2a for $Co_2(CO)_6$, we have to take into account that tungsten d orbitals are more diffuse than those of cobalt. Besides obtaining the bonding and antibonding combi-

(4) Albright, T. A.; Burdett, J. K.; Whangbo, M.-H. *Orbital Interactions in Chemistry*; Wiley Interscience: New York, 1985.

**8**

**9**

substituents) are bent back, these two sets lose their degeneracy. The $\pi$ and $\pi^*$ orbitals in the plane of the molecule mix with other orbitals,[1] $\pi^*$ being stabilized and $\pi$ destabilized. They thus become better suited for interaction with metal fragments orbitals, both in energy and in overlap terms. The four resulting orbitals of bent acetylene are shown in the right side of Figure 2.

The four bonding combinations between acetylene and metal fragment orbitals are represented in **10a–d**. These

nation between each orbital in each $WCl_3$ fragment, considerable mixing between the two e sets occurs.

This dimeric $W_2Cl_6$ unit will develop into two face-sharing octahedra upon interacting with the three bridging ligands, two $NH_2^-$ and an acetylene, **7**. Let us do it in two steps. First we add two $NH_2^-$ units. The symmetry of the fragment is now $C_{2v}$. There are four filled orbitals in the bridging ligands that will donate electrons to empty orbitals in $W_2Cl_6$. The bonding combinations are shown in **9a–d**.

**10**

may be identified with the orbitals in Figure 2 in the following way: **10a** $\approx$ $1a_1$, **10b** $\approx$ $1b_1$, **10c** $\approx$ $1b_2$, and **10d** $\approx$ $1a_2$. Note that the $a_2$ orbital, $1a_2 \approx$ **10d**, is empty. There are only three bonding electron pairs to make four W–C bonds. On the other hand, the two highest occupied molecular orbitals can be considered to represent M–M bonds, the HOMO a $\pi$-type one and the other a $\sigma$ bond. The HOMO–LUMO gap is small, and a second-order Jahn–Teller distortion is expected. Rotation of acetylene destroys the symmetry planes, retaining only the twofold axis. The HOMO ($a_1$) and the LUMO ($a_2$) become of the same symmetry (a in $C_2$) and can mix. So they do, with resultant stabilization of the HOMO and the molecule as a whole. A schematic representation of the new W–C bond strengthening interaction, which comes into play as twisting occurs, is shown in **11** from a top view. The sta-

**11**

The frontier orbitals of the $W_2(\mu\text{-}NH_2)_2Cl_6^{2-}$ fragment are shown in the left side of Figure 2. Here we represent its interaction with an acetylene molecule in perpendicular geometry. Before looking at further details, let us review the acetylene frontier orbitals. Linear acetylene has two $\pi$ and two $\pi^*$ orbitals. When the hydrogens (or other
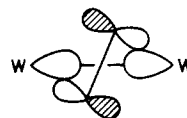
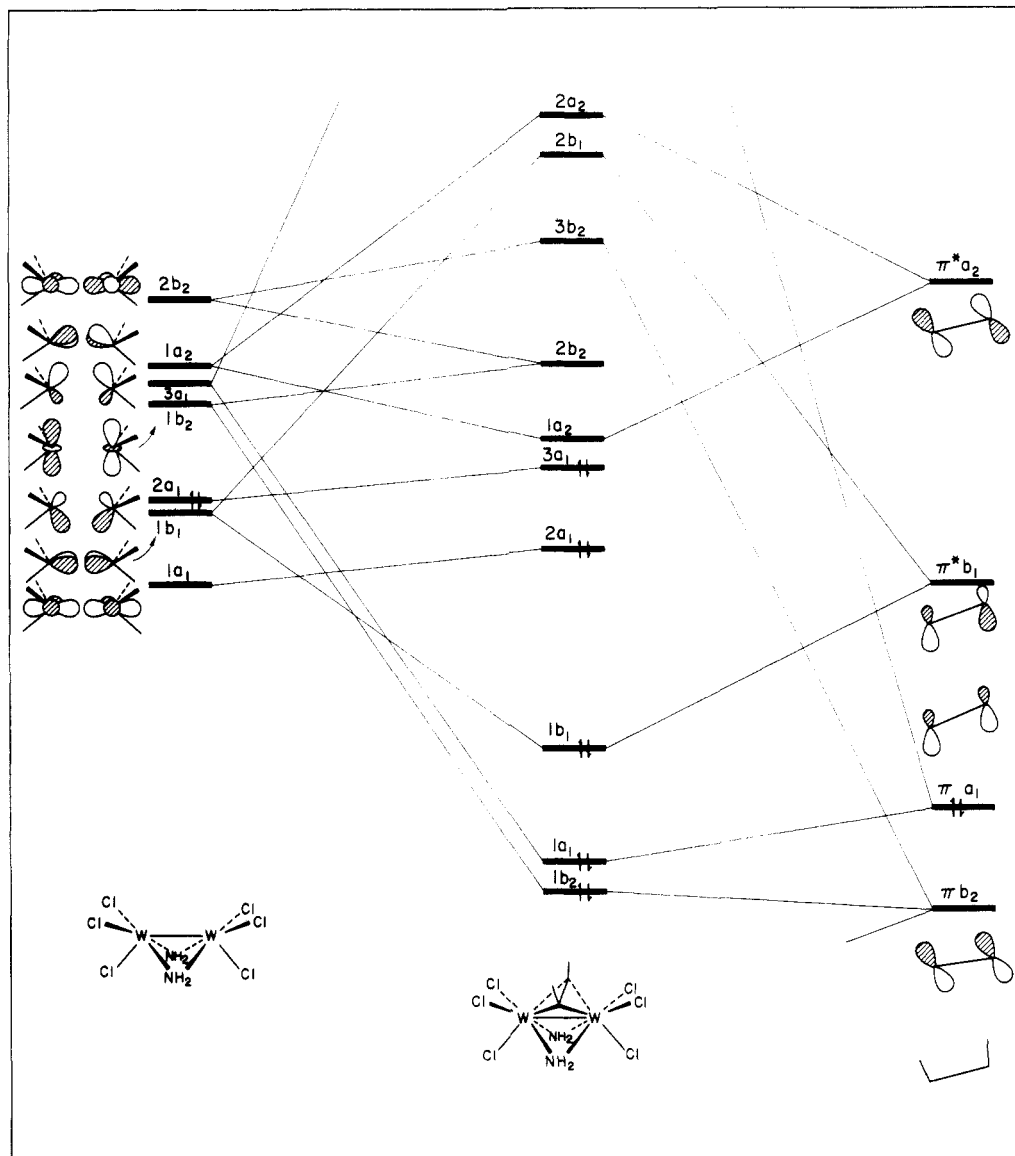bilizing mixing is of orbitals $1a_2$ and $3a_1$ of the composite

**Figure 2.** Interaction diagram for $W_2(NH_2)_2(C_2H_2)Cl_6^{2-}$ with the acetylene in a perpendicular geometry.

molecule. But the "active" parts of this interaction can be thought of as being derived from acetylene and $W_2$ fragment orbitals, $a_2(\pi^*)$ at right and $2a_1$ at left in Figure 2, respectively.

The Walsh diagram (Figure 3a) shows this stabilizing interaction in some detail. Note the repulsion of $3a_1$ and $1a_2$ as twisting proceeds. Actually the two highest occupied levels are stabilized with twisting—there is an avoided crossing, and it is actually $2a_1$ which overlaps better with $1a_2$. Lower levels behave differently, and we must examine the components of the total energy in some detail.

In figure 3b we reproduce the calculated potential energy curve for the $Cl_6$ compound, $d^3$, $d^3$, with its somewhat shallow minimum at 26° rotation. We also give the energy curve for the six electrons in the three mainly d levels, marked "d electrons", and the total energy curve for all the lower levels, marked $d^0$, $d^0$ core. The latter curve is a nice calibration for the composite energetic preference of core levels, steric effects, and metal–carbon bonding.

Note that the $d^0$, $d^0$ core curve favors 0° and 90°, i.e., parallel and perpendicular acetylene bonding. On top of that behavior, which we will see maintained and perturbed in interesting ways, one finds the large effect of the second-order Jahn–Teller stabilization, the "d electron" curve, driven largely by the HOMO. This bonding effect favors

a twisted acetylene and wins out, but barely so, over the core effect.

**Bonding in $W_2(NH_2)_2(C_2H_2)Cl_4H_2^{2-}$ and the Origins of the Rotation**

Let us compare those results to what happens when two of the chlorines are replaced by hydrogens, lowering the molecule symmetry to $C_2$. The first consequence is a lowering in energy of most frontier orbitals in $W_2$-$(NH_2)_2Cl_4H_2^{2-}$ compared to $W_2(NH_2)_2Cl_6^{2-}$. This comes from loss of antibonding W–Cl character as two chlorine atoms are removed. The second is a distortion of the orbitals, to which we will return in a moment.

The interaction diagram between this fragment and acetylene is very similar to that shown in Figure 2. The HOMO–LUMO gap is still very small, indicative of a second-order Jahn–Teller distortion. We saw (Figure 1) that in $W_2(NH_2)_2(C_2H_2)Cl_4H_2^{2-}$ there is a strong preference of acetylene for a specific distorted geometry (rotation 135°) in contrast to the situation in the hexachloride complex. Let us look at the Walsh diagram (Figure 4). Maximum stabilization of the highest occupied orbitals is achieved for rotations of 45° and 135°. There are several avoided crossings which probably explain the strange shape
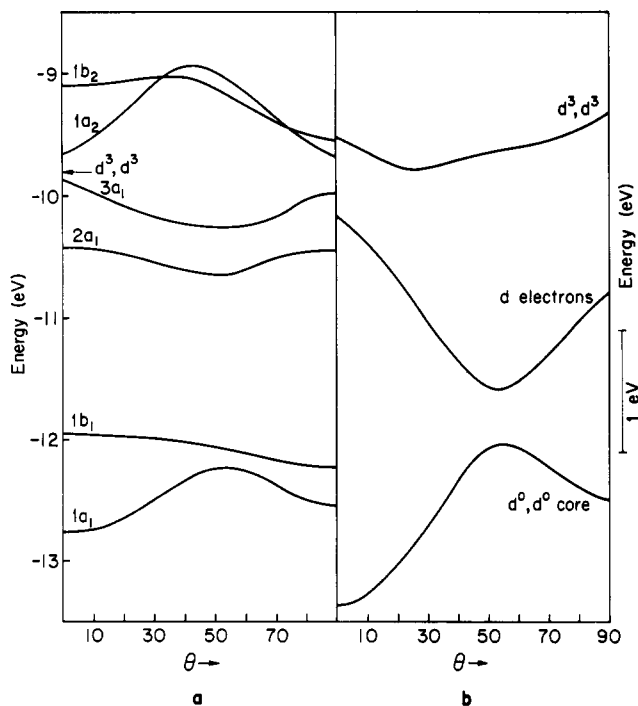
**Figure 3.** (a) Walsh diagram for rotation of acetylene in $W_2$-$(NH_2)_2(C_2H_2)Cl_6{}^{2-}$. (b) Total energy curves for the experimental $d^3$, $d^3$ configuration, for a "$d^0$, $d^0$" core configuration, and the difference between the two, labeled "d electrons".

observed for the total energy curve (Figure 1).

Stabilization is provided by mixing of empty $\pi^*(a_2)$ of acetylene. This orbital interacts increasingly strongly with the "$2a_1$" fragment orbital of $W_2(NH_2)Cl_4H_2$ as rotation occurs. Figure 5 helps to visualize this. It shows the "$2a_1$" fragment orbital; above it the unrotated $\pi^*(a_2)$—little overlap, nodal plane mismatch—and below it the rotated $\pi^*(a_2)$, which can be seen to have a superb overlap with $2a_1$. The new HOMO is mainly the bonding combination of these two orbitals.

Note that this better overlap is just an illustration of the operation of the second-order Jahn–Teller theorem at work. It would provide mixing and therefore stabilization for rotation of the acetylene toward *or* away from the hydride ligands.

Figure 4b gives the decomposition of the total energy. The "d electrons" curve shows that interaction between metal d orbitals and acetylene orbitals favors either a 45° rotation or a 135° rotation. However, there is a preference for the 135° one, when we look at the total $d^3$–$d^3$ energy. This means that the answer must lie in the lower energy orbitals. Indeed the $d^0$, $d^0$ core curve, the "core" energy, is very different for $W_2(NH_2)_2(C_2H_2)Cl_4H_2{}^{2-}$ than for the $Cl_6$ case. There is now only one large hump at $\theta \approx 50°$, and the other maximum, around $\theta \approx 135°$, is gone.

In our search for a controlling orbital we focus on the lowest orbital in Figure 4a, $1a_1$. On comparing the variation in energy in this orbital with the $d^0$, $d^0$ core curve, we can see that it is an important orbital in determining the shape of the $d^0$ curve. We did not find another orbital showing such an asymmetry toward 45° and 135° rotations. At a perpendicular geometry, this molecular orbital is 82% localized on the acetylene. It is bonding between W and C but antibonding between W and Cl. A schematic representation of this orbital is shown in **12**.

If we rotate the acetylene so that the carbon atoms point toward the chlorines, an antibonding interaction will develop, and the orbital energy will rise. If we rotate the acetylene by 135°, the carbon atoms are far away from
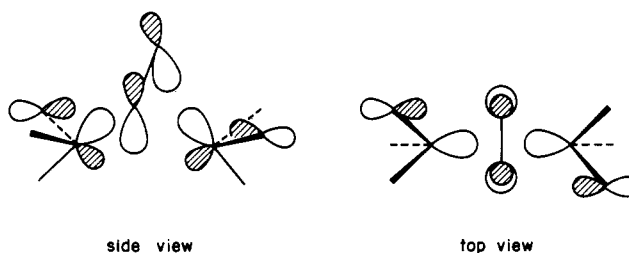


**12**

chlorines; they point instead to the hydrogens. As there is no hydrogen participation in this orbital, its energy should stay the same. This is not exactly so, because other orbitals will mix as rotation proceeds, but this is a minor effect.

Let us go back to parts a and b of Figure 3. We think the same effect is the one responsible for resistance to further deformation in the $W_2(NH_2)_2(C_2H_2)Cl_6{}^{2-}$ species. Note first that the lowest $a_1$ level moves in energy just as the $d^0$, $d^0$ core curve does. Secondary antibonding interactions between acetylene carbons and chloride orbitals create energy humps at $\sim 90°$ *and* 135° rotations. The second-order Jahn–Teller driven energy of the six electrons in the d levels overcomes these, but not by much.

The secondary repulsion argument was probed further in the following way. The hexachloro compound was examined again, but now setting equal to zero the matrix elements between the carbons and two of the chlorides, $Cl^*$ in **13**. The resulting potential energy curve resembles
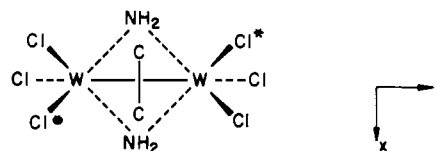


**13**

closely that for $W_2(NH_2)_2(C_2H_2)Cl_4H_2{}^{2-}$, with a single deep minimum at $\theta \approx 130°$. Conversely taking the $Cl_4H_2$ system, with its single minimum, and dropping two further C–Cl interactions symmetrized the energy curve. We consider the C–Cl secondary repulsion argument confirmed by these numerical experiments.

If the secondary interaction is repulsive with $\pi$-donor substituents, could it be made attractive with $\pi$-acceptor ligands such as carbonyls? We had hoped this would happen in **14**, with an expected deeper minimum for an
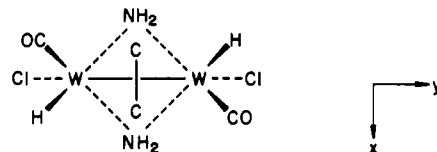


**14**

acetylene twisted toward eclipsing the carbonyls. Unfortunately, this did not occur in the calculations—the two minima at $\theta \approx 45°$ and 135° remained of approximately equal depth.

Returning to the parent system, we probed for possible steric effects in several ways. First we put a methyl group on each bridging amide, in the worst position, toward the acetylene. Essentially the same rotation curves were found.
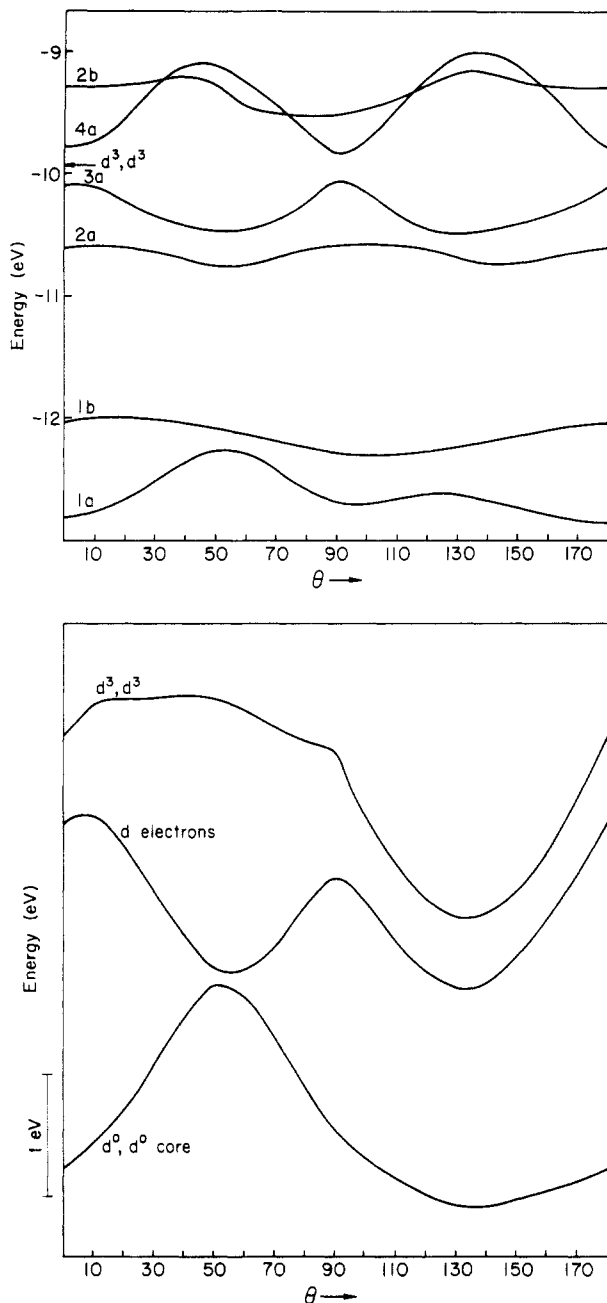
**Figure 4.** (a) Walsh diagram for rotation of acetylene in $W_2$-$(NH_2)_2(C_2H_2)Cl_4H_2{}^{2-}$. (b) Total energy curve decomposition. See Figure 3 caption for details.

So the amide substituents do not cause the acetylene to rotate[5].

Back in Figure 1 is the computed total energy for the pyridine complex. Note the minimum occurs at $\theta \approx 150°$, while electronically one might have expected 135°. Looking carefully at the complex, we see that there is a close contact between an acetylene hydrogen and one of pyridine $\alpha$-hydrogens at 135° rotation. We can increase that distance by distorting the H–C–C–H group, making that dihedral angle greater than 0°. This was done, at $\theta$ = 135° and 150°. The computed curves were rather flat, but for about a 40° torsion angle (H–C–C–H) the lower $\theta$ angle, a geometry close to the experimental one, was preferred.



**Figure 5.** At top—the $\pi^*(a_2)$ orbital of an acetylene in a perpendicular orientation ($\theta = 90°$). In the middle—the $2a_1$ valence orbital of $W_2(NH_2)_2Cl_4H_2$. At bottom—the same $\pi^*(a_2)$ acetylene orbital as a top, but now rotated by 45°: i.e., $\theta$ = 45 or 135°.

In summary we have traced the origins of the unusual rotation of the acetylene in this dinuclear complex to an interesting interplay of a core stereoelectronic asymmetry, due to metal–halide $\pi$ bonding, on which is superimposed an electronic d-block tendency to rotate away from perpendicular. It will be interesting to seek further derivatives in this series, substituted at the metal.

(5) We have also tried to understand the small twist present[3] in $W_2Cl_2(NMe_2)_4(C_2H_2)(py)_2$ but have so far not been able to include realistic enough ligands to model the acetylene conformation in this sterically constrained system.
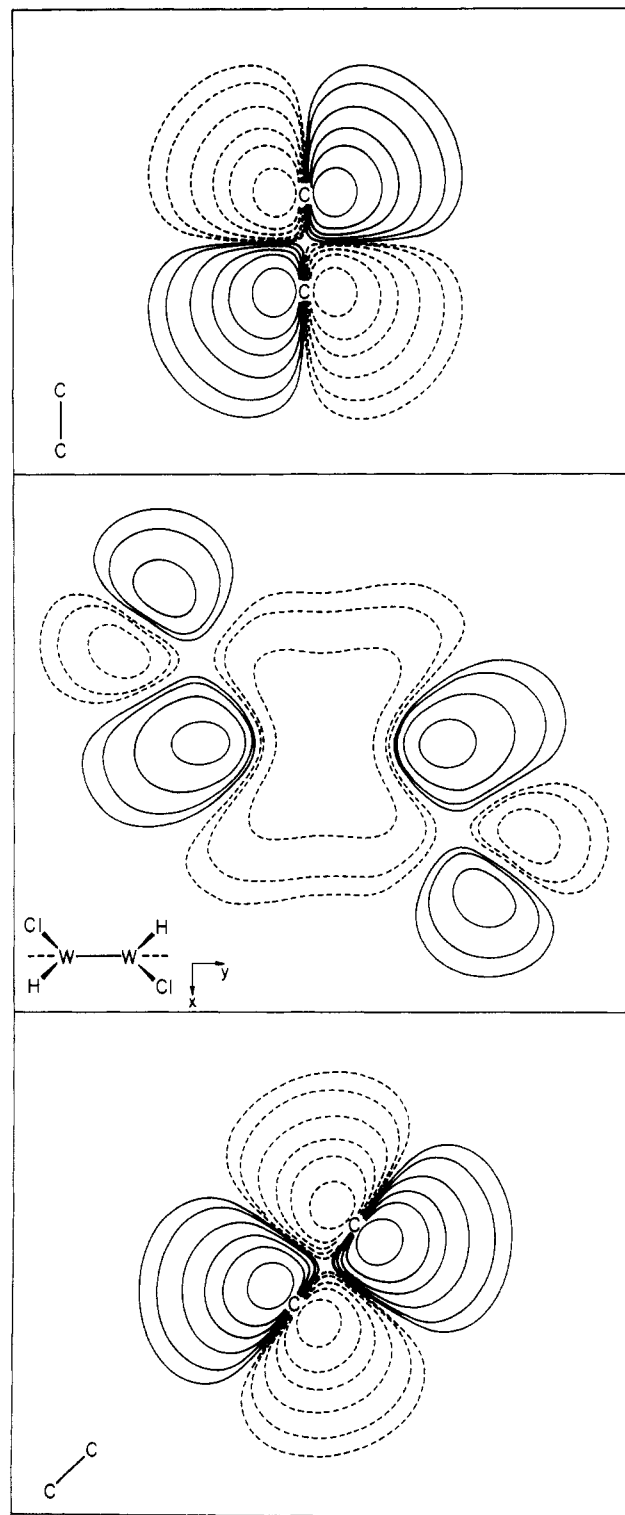
for a Fulbright grant which made her stay at Cornell possible and the National Science Foundation for its support of this work through research Grant CHE 84-06119. We were stimulated to do this work through the friendly communication of his group's results by Malcolm Chisholm.

## Appendix

Calculations were made by using the extended Hückel method,[1] with weighted $H_{ij}$'s. The parameters for W, C, H, N, and O were taken from previous work.[1] Geometries were modelled after the X-ray determined structure of $W_2(NMe_2)_2(C_2Me_2)Cl_4(py)_2$.[1] The following bond distances were used: $C_{ac}-C_{ac} = 1.376$ Å, $C_{ac}-H = 1.09$ Å, W–Cl = 2.40 Å, W–H = 1.70 Å, W–N = 2.18 Å, N–H = 1.02 Å, and W–W = 2.436 Å. An octahedral environment around each tungsten was kept. The acetylene was allowed to rotate at a distance 1.87 Å above the W–W axis.

# Cationic 2-Azaallenylidene Complexes of Chromium and Tungsten. Complexes with a Novel Metallaheterocumulene System[1]

Friedrich Seitz, Helmut Fischer,* Jürgen Riede, and Jürgen Vogel

*Anorganisch-chemisches Institut der Technischen Universität München, D-8046 Garching, Federal Republic of Germany, and Physikalisch-chemisches Institut der Technischen Universität München, D-8046 Garching, Federal Republic of Germany*

The reaction of $(CO)_5M[C(OEt)N=CR_2]$ with $BF_3$ yields 2-azaallenylidene complexes $[(CO)_5M=C=N=CR_2]BF_4$ (M = Cr ([3]$BF_4$), W ([4]$BF_4$); $CR_2 = C(C_6H_4Br-4)_2$ (a), $CPh_2$ (b), $C(C_6H_4OMe-4)_2$ (c), $C(C_6H_4)_2O$ (d), $C(2,4,6-C_6H_2Me_3)_2$ (e), $C(CMe_3)_2$ (f)). The abstraction of $Cl^-$ from $(CO)_5Cr—C≡N—CCl_3$ by $AlCl_3$ gives $[(CO)_5Cr—C=N=CCl_2]AlCl_4$ ([3a]$AlCl_4$). IR, $^{13}C$ NMR, and electronic spectra reveal the high degree of electron delocalization within the metallaheterocumulene system. The structure of [3d]-$BF_4·CH_2Cl_2$ has been determined by an X-ray diffraction analysis (crystal data: monoclinic, space group $P2_1/c$, a = 15.811 (4) Å, b = 12.657 (4) Å, c = 12.966 (3) Å, $\beta$ = 111.98 (2)°, and Z = 4). The Cr–C–N–C fragment is almost linear (Cr–C–N = 179.0 (5)°; C–N–C = 171.1 (5)°) and allows the formation of two orthogonal $\pi$-systems. Both C–N distances (118.4 (7) and 134.3 (7) pm, respectively) differ significantly. Therefore, the complexes are best described as resonance hybrids of the two limiting structures A and B: the 2-azaallenylidene complex A and the carbocationic isonitrile complex B. [3d]$BF_4$ reacts with $Me_3N^+–O^-$ to yield the ketone $O=C(C_6H_4)_2O$. On near-UV irradiation of [3b]$BF_4$ and [3d]$BF_4$, the olefins $R_2C=CR_2$ ($CR_2 = CPh_2$, $C(C_6H_4)_2O$) are formed.

Heterocumulene systems can act as nonbridging ligands in transition-metal complexes in one of the following ways: $\eta^2$ side on, as in several ketene complexes[2-5] and a 1,3-diphosphaallene complex;[6] $\eta^3$ side on, as in a 1-azaallyl complex[7] and a 1,3-diphosphaallyl complex;[8] singly bonded end on, as in ketenyl,[9,10] keteniminyl,[11] and 2-azaallenyl complexes;[12] and multiply bonded end on, in a fashion analogous to allenylidene complexes.[13] This latter type of bonding seems particularly interesting, as a new, longer cumulene system is created thereby, with the metal now being part of the cumulene system.

The extended $\pi$-system in these complexes lends itself to studying the effects of electron delocalization on structure and reactivity, which is an important field with regard to catalytic and biological processes (e.g., electron transfer). However, only a few metal heterocumulene systems are known, e.g., 1-azavinylidene complexes,[7,14] a 1-phosphavinylidene complex,[15] and a oxapropatrienylidene complex.[16] Therefore we decided to develop more general synthetic routes to metal heterocumulene systems and chose 2-azaallenylidene complexes, i.e., complexes that

(1) Metallaheterocumulenes. 5. For part 4 see: Fischer, H.; Seitz, F.; Riede, J. *Chem. Ber.* **1986**, *119*, 2080.

(2) Miyashita, A.; Shitara, H.; Nohira, H. *Organometallics* **1985**, *4*, 1463.

(3) Herrmann, W. A.; Plank, J.; Ziegler, M. L.; Weidenhammer, K. *J. Am. Chem. Soc.* **1979**, *101*, 3133.

(4) Casey, C. P.; O'Connor, J. M. *J. Am. Chem. Soc.* **1983**, *105*, 2919.

(5) Moore, E. J.; Straus, D. A.; Armantrout, J.; Santarsiero, B. D.; Grubbs, R. H.; Bercaw, J. E. *J. Am. Chem. Soc.* **1983**, *105*, 2068.

(6) Akpan, C. A.; Meidine, M. F.; Nixon, J. F.; Yoshifuji, M.; Toyota, K.; Inamoto, N. *J. Chem. Soc., Chem. Commun.* **1985**, 946.

(7) Green, M.; Mercer, R. J.; Morton, C. E.; Orpen, A. G. *Angew. Chem.* **1985**, *97*, 422; *Angew. Chem., Int. Ed. Engl.* **1985**, *24*, 422.

(8) Appel, R.; Schuhn, W.; Knoch, F. *Angew. Chem.* **1985**, *97*, 421; *Angew. Chem., Int. Ed. Engl.* **1985**, *24*, 420.

(9) Kreissl, F. R.; Eberl, K.; Uedelhoven, W. *Angew. Chem.* **1978**, *90*, 908; *Angew. Chem., Int. Ed. Engl.* **1978**, *17*, 859.

(10) Kreissl, F. R.; Eberl, K.; Uedelhoven, W. *Chem. Ber.* **1977**, *110*, 3782.

(11) Aumann, R.; Heinen, H. *Chem. Ber.* **1985**, *118*, 952.

(12) Seitz, F.; Fischer, H.; Riede, J. *J. Organomet. Chem.* **1985**, *287*, 87.

(13) Bruce, M. I.; Swincer, A. G. *Adv. Organomet. Chem.* **1983**, *22*, 59.

(14) Keable, H. R.; Kilner, M. *J. Chem. Soc., Dalton Trans.* **1972**, 153.

(15) Cowley, A. H.; Norman, N. C.; Quashie, S. *J. Am. Chem. Soc.* **1984**, *106*, 5007.

(16) Berke, H.; Härter, P. *Angew. Chem.* **1980**, *92*, 224; *Angew. Chem., Int. Ed. Engl.* **1980**, *19*, 225.